macokinetics have not been well understood, and the effect of another concomitantly administered calcineurin inhibitor, tacrolimus, on everolimus pharmacokinetics have not been sufficiently enough evaluated.

In this study, we administered everolimus by different routes namely, intraintestinally, intraportally and intravenously, and separately evaluated the effect of intestinal and hepatic extraction on the pharmacokinetics of everolimus in rats. Next, we examined the effects of cyclosporine and tacrolimus on the first-pass extraction of everolimus. Although it should be noted that there are some peculiarities of drug metabolism in rats when bioavailability or drug-drug interactions are extrapolated to humans, the findings presented here could be helpful to understand the bioavailability of everolimus and interaction mechanisms of calcineurin inhibitors in humans, because injectable formulation of everolimus is not on the market and its bioavailability in humans is unknown.

Materials and Methods

Materials: Everolimus was a gift from Novartis Pharma AG (Basel, Switzerland) and it was in microemulsion and injection formulations. Tacrolimus injection solution (Prograf injection, 5 mg/mL) was obtained from Astellas Pharma Inc. (Tokyo, Japan). Cyclosporine (Sandimmun injection, 50 mg/mL) was obtained from Novartis Pharma KK (Tokyo, Japan). 32-Desmethoxyrapamycin was obtained from Wyeth (Madison, NJ). All other chemicals used were of the highest purity available.

Animals: Male Wistar/ST rats weighing 220 to 260 g (8 week old) were used for in the vivo study. Before the experiment, rats were fasted overnight, but given free access to water. Animals were anesthetized with sodium pentobarbital (1 mg/kg i.p.). Supplemental doses of pentobarbital were administered as required. Body temperature was maintained with appropriate heating lamps. The animal experiments were performed in accordance with the Guidelines for Animal Experiments of Kyoto University.

Pharmacokinetic studies in rats: In each experiment, the femoral artery was cannulated with a polyethylene tube (PE-50; BD Biosciences, San Jose, CA) filled with heparinized saline (50 U/mL) for blood sampling. In the experiments for intravenous administration, the femoral vein was cannulated, and everolimus was administered from the femoral vein. In separate experiments for intraportal administration, portal vein was cannulated with a polyethylene tube (PE-10) with a 26 G needle, and everolimus was administered intraportally for 60 min using an infusion pump at a rate of 2.2 mL/hr. In separate experiments for intraintestinal administration of everolimus, the abdominal cavity was opened via a midline incision, and the upper site of the duodenum was exposed to administer everolimus. To examine effect of intraintestinal administration of 5 mg/kg cyclosporine or 1 mg/kg tacrolimus, the abdominal cavity was opened via a midline incision, and the upper site of the duodenum was exposed to administer each drug. Everolimus was administered intravenously or intraintestinally at 10 min after intraintestinal administration of cyclosporine, tacrolimus or saline (control). Blood samples were collected from the femoral artery at 5, 15, 30, 60, 120, 180 and 240 min after the start of the administration of everolimus. Samples were placed into EDTA anticoagulant tubes.

To separately evaluate the influence of calcineurin inhibitors on the intestinal and hepatic first-pass effects of everolimus, cyclosporine (5 mg/kg) and tacrolimus (1 mg/kg) was intraintestinally administered 10 min before everolimus administration, and everolimus were administered intraportally or intraintestinally for 60 min using an infusion pump at a rate of 2.2 mL/hr. Blood samples were collected from the femoral artery at 5, 15, 30 and 60 min after the beginning of everolimus administration. Samples ware placed into EDTA anticoagulant tubes.

Analytical methods: Whole blood samples (150 μL) were transferred to 13 mL glass tubes and spiked with the internal standard (10 μL of 300 ng/mL of 32-desmethoxyrapamycin in blood). The analytical method for everolimus from the whole blood samples was performed by a previous method for sirolimus using high performance liquid chromatography with tandem mass spectrometry (LC/MS/MS).[14] Mass analysis was performed using a triple quadrupole mass spectrometer (API4000, Applied Biosystems Japan Ltd., Tokyo, Japan) equipped with an electrospray ionization interface and operated in the positive ion mode. The ion transitions monitored were the mass-to-change ratio (m/z) 975.6→908.6 for everolimus and m/z 901.5→834.7 for the internal standard. The lower limit of quantification for everolimus was 0.5 ng/mL.

Pharmacokinetic analysis: The pharmacokinetic parameters of everolimus, the area under the blood concentration-time curve from time zero to infinity (AUC), total body clearance (CL), volume of distribution at steady-state (Vd_{ss}) and half-life ($T_{1/2}$) were calculated with the software WinNonlin version 4.0.1 (Pharsight Co. Mountain View, CA) using the two-compartment model for the dose-dependent study and non-compartment model for other studies. Maximum concentration (C_{max}) and time of maximum concentration (T_{max}) were obtained from concentration-time curve of everolimus. The bioavailability after intraintestinal (F) or intraportal administration (F_h, hepatic availability) was calculated using the dose-normalized AUC after intraintestinal or intraportal administration divided by the dose-normalized AUC after intravenous administration, respectively. The apparent intestinal availability was obtained by dividing F by F_h. The area under the blood concentration-time curve

for 60 min (AUC_{0-60}) values of everolimus after intraportal and intraintestinal infusion were calculated by the trapezoidal method.

Statistical analysis: Values are expressed as means ± standard error of the mean (SE) for n experiments, except for that T_{max} is shown as median (min-max). The dose dependence of CL and Vd_{ss} was examined using the linear regression. Comparison of mean blood concentrations among three groups was performed by the repeated measures ANOVA with the post-hoc Dunnett test. The statistical significance of mean pharmacokinetic parameters among three groups was performed using Dunnett test following ANOVA. The statistical analysis for the distribution of T_{max} was performed using Kruskal-Wallis test. Difference was considered significant at $p<0.05$.

Results

Dose dependency of everolimus pharmacokinetics: We first examined the dose proportionality of everolimus after intravenous administration (0.2, 0.5 and 1 mg/kg). The everolimus concentration profile showed a two-phase decline (**Fig. 1**). The CL did not correlate with the dose ($P=0.096$), while Vd_{ss} significantly correlated with the dose from 0.2 to 1.0 mg/kg ($P<0.05$, **Table 1**).

First-pass extraction of everolimus by the intestine and liver: To clarify the contribution of the intestine and liver to the first-pass effect of everolimus, 0.5 mg/kg of everolimus was administered intraintestinally, intraportally and intravenously (**Fig. 2**). The bioavailability after intraportal and intraintestinal administration were 48.0% and 21.2%, respectively, assuming that the pharmacokinetics of everolimus was linear in this condition (**Table 2**). The values of intestinal and hepatic availability were calculated as 44.2% and 48.0%, respectively.

Effect of calcineurin inhibitors on the pharmacokinetics of everolimus: The pharmacokinetics of everolimus after intravenous and intraintestinal administration with or without the pre-administration of cyclosporine or tacrolimus was evaluated. After the intravenous administration (0.2 mg/kg), the everolimus concentration was not significantly elevated with each calcineurin inhibitor (**Fig. 3A**). The AUC and CL values after the intravenous administration with cyclosporine were significantly changed compared with those in the control, and those with tacrolimus were slightly changed (**Table 3**). When everolimus was administered intrain-

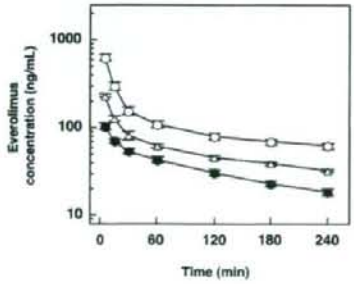

Fig. 1. Time-concentration profiles of everolimus after intravenous administration
Blood concentrations of everolimus at a dose of 1 mg/kg (open circles; n=5), 0.5 mg/kg (open triangles; n=5) and 0.2 mg/kg (closed circles; n=6) were plotted. Each line shows a simulation curve fitted to the two-compartment model. Each point shows the mean ± SE.

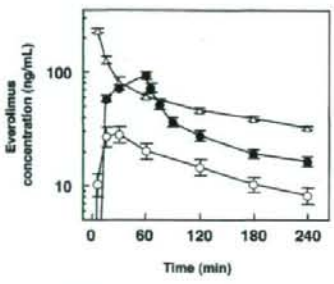

Fig. 2. Time-concentration profiles of everolimus after intravenous, intraportal and intraintestinal administration
Blood concentration of everolimus following intraintestinal (open circles; n=5), intraportal (closed circles; n=6) or intravenous (open triangles; n=3) administration at a dose of 0.5 mg/kg were plotted. Each point shows the mean ± SE.

Table 1. Total body clearance (CL) and volume of distribution at steady-state (Vd_{ss}) after intravenous administration at a dose of 0.2, 0.5 or 1 mg/kg by the two-compartment model

Dose (mg/kg)	CL (L/hr/kg)	Vd_{ss} (L/kg)
0.2 (n=6)	0.96±0.06	3.29±0.31
0.5 (n=5)	1.25±0.04	5.55±0.63
1.0 (n=5)	1.19±0.11	6.03±1.12

Each point shows the mean ± SE.

Table 2. Area under the blood concentration-time curve (AUC) and bioavailability following intravenous, intraportal or intraintestinal administration of everolimus in rats

Administration Route	Dose (mg/kg)	AUC (mg·hr/L)	Bioavailability (%)
Intravenous (n=3)	0.5	0.433±0.027	100
Intraportal (n=6)	0.5	0.208±0.016	48.0
Intraintestinal (n=5)	0.5	0.092±0.015	21.2

Each value shows the mean ± SE.

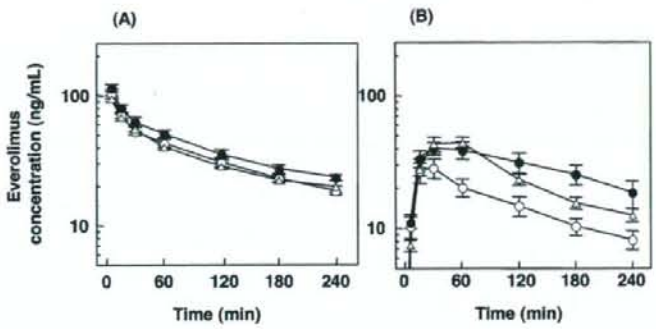

Fig. 3. Effect of calcineurin inhibitors on blood concentration of everolimus in rats
Blood concentrations of everolimus following intravenous (0.2 mg/kg, panel A) or intraintestinal (0.5 mg/kg, panel B) administration were plotted. Saline (open circles; control, n=6 for panel A, n=5 for panel B), 1 mg/kg of tacrolimus (open triangles; n=5 for panel A, n=4 for panel B) or 5 mg/kg of cyclosporine (closed circles; n=5 for panel A, n=5 for panel B) were intraintestinally administered 10 min before everolimus administration. Each point shows the mean±SE.

Table 3. Pharmacokinetic parameters of everolimus after intravenous and intraintestinal administration with or without administration of cyclosporine and tacrolimus by the non-compartment model

Parameter	Control	Cyclosporine	Tacrolimus
Intravenous administration (0.2 mg/kg)			
n	6	5	5
AUC (mg·hr/L)	0.217±0.016	0.263±0.013*	0.226±0.010
CL (L/hr/kg)	0.945±0.068	0.768±0.036*	0.892±0.038
Vd_{ss} (L/kg)	3.47±0.38	2.86±0.24	3.55±0.24
$T_{1/2}$(hr)	3.65±0.24	3.70±0.14	3.97±0.17
Intraintestinal administration (0.5 mg/kg)			
n	5	5	4
AUC (mg·hr/L)	0.092±0.015	0.194±0.045	0.137±0.012
T_{max} (min)	30 (15–30)	60 (30–60)	60 (30–60)
C_{max} (ng/mL)	28.9±2.7	41.7±4.6	44.5±5.1
F (%)	16.9	29.5	24.3

Each value shows the mean±SE. *$p<0.05$ compared with the control.

testinally (0.5 mg/kg), blood concentrations of everolimus tended to elevate by pre-administration of both cyclosporine and tacrolimus (**Fig. 3B**). The AUC value with cyclosporine was doubled, but did not reach statistical significance (**Table 3**). The F value of everolimus was calculated as 16.9% in the control, and increased to 29.5% and 24.3%, respectively, with pre-administration of cyclosporine and tacrolimus (**Table 3**).

Effect of calcineurin inhibitors on the intestinal and hepatic first-pass extraction of everolimus: To further examine the effect of calcineurin inhibitors on the intestinal and hepatic extraction of everolimus, everolimus (0.5 mg/kg) was administered intraportally or intraintestinally at a rate of 2.2 mL/hr for 60 min after calcineurin inhibitors were administered intraintestinally. After the intraportal administration, blood concentrations of everolimus in the cyclosporine and tacrolimus groups were not significantly elevated compared with that of the control (**Fig. 4A**). The $AUC_{0\text{-}60}$ values in the cyclosporine and tacrolimus groups were not significantly increased after intraportal infusion (**Table 4**). On one hand, blood concentrations of everolimus after the intraintestinal infusion were significantly elevated in the cyclosporine group compared with control (**Fig. 4B**), and the $AUC_{0\text{-}60}$ value in the cyclosporine group was significantly increased by about 3-fold (**Table 4**). Blood concentrations of everolimus and the $AUC_{0\text{-}60}$ value in the tacrolimus group were not significantly changed compared with the control (**Fig. 4B**, **Table 4**).

Discussion

Everolimus is eliminated from the body by the metabolism of CYP3A subfamily,[10] and CYP3A4 as well as CYP3A5 are known to be expressed in human liver and intestine.[15] In adult male rats, CYP3A2, CYP3A9, CYP3A18, CYP3A1/23 and CYP3A62 are expressed in livers, and CYP3A62 as well as CYP3A9 and CYP3A18 are detected in the intestinal tract.[16] Cao *et al.*[17] suggested that a rat model could not be used to predict drug metabolism or oral bioavailability in humans, since the two species exhibit distinct expression levels and patterns for metabolizing enzymes in the intestine. On one hand, the bioavailability of tacrolimus and cyclosporine, typical substrates of CYP3A subfamily, in humans are poor and varies from 4% to 89% (mean approximately 25%) and from <5% to 89% (average approximately 30%, classical formulation), respectively,[18,19] and the reported bioavailability in rats are similar to the mean values in humans.[20,21] Everolimus has been on the market only as an

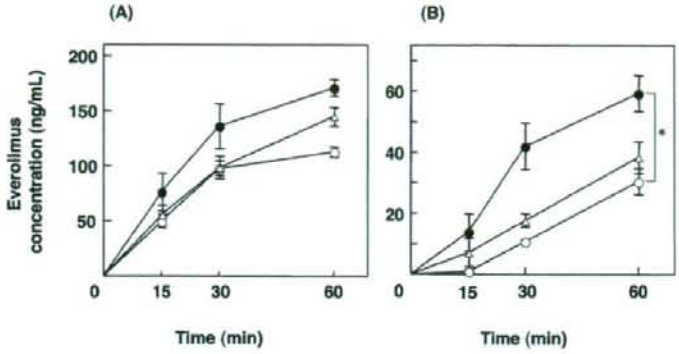

Fig. 4. Time-concentration profile of everolimus after intraportal infusion (panel A) and intraintestinal infusion (panel B) at a dose of 0.5 mg/kg

Saline (open circles; control, n = 5 for panel A, n = 3 for panel B), 1 mg/kg of tacrolimus (open triangles; n = 5 for panel A, n = 4 for panel B) or 5 mg/kg of cyclosporine (closed circles; n = 3 for panel A, n = 4 for panel B) were intraintestinally administered 10 min before everolimus administration. Each point shows the mean ± SE. *$p < 0.05$ compared with control.

Table 4. Area under the blood concentration-time curve for 60 min (AUC_{0-60}, mg·hr/L) values of everolimus after intraportal and intraintestinal infusion with or without administration of cyclosporine and tacrolimus

	Control	Cyclosporine	Tacrolimus
Intraportal	0.084 ± 0.004 (n = 5)	0.113 ± 0.014 (n = 3)	0.087 ± 0.007 (n = 5)
Intraintestinal	0.012 ± 0.001 (n = 3)	0.034 ± 0.005* (n = 4)	0.018 ± 0.002 (n = 4)

Each value shows the mean ± SE. * $p < 0.05$ compared with the control.

oral formulation, and there is no information about its bioavailability in humans. Therefore, we investigated the effect of intestinal and hepatic first-pass extraction on the pharmacokinetics of everolimus in rats to understand the bioavailability in humans, although the species difference should be taken into consideration.

To evaluate the pharmacokinetic parameters of everolimus, we first examined its dose proportionality. The CL was constant, but Vd_{ss} significantly correlated with the dose from 0.2 to 1.0 mg/kg (**Table 1**). Since everolimus was reported to exhibit moderate non-linear binding to red blood cells,[22] the CL as well as Vd_{ss} may increase as the blood concentrations increased. In stable renal transplant patients, dose-normalized AUC values were not significantly different for doses in the range 2.5–25 mg but were higher at the 0.75 mg dose.[3] Considering that the blood concentration profile after intravenous administration well fitted to the two-compartment model at each dose, everolimus pharmacokinetics can be regarded as linear in a relatively small concentration range. Since the everolimus concentration was between 10 and 100 ng/mL after intravenous administration of 0.2 mg/kg, we carried out the following experiments in this concentration range, assuming the pharmacokinetic linearity.

To quantitatively evaluate the intestinal and hepatic first-pass extraction, everolimus was administered intravenously, intraportally and intraintestinally at a dose of 0.5 mg/kg (**Fig. 2**). As a result, the intestinal and hepatic availability were 44.2% and 48.0%, respectively, showing both intestine and liver function to be absoption barriers to everolimus. These results were consistent with a previous report that 50% of everolimus was metabolized in the intestinal mucosa in an *in situ* rat jejunum administration study at a dosage of 0.5 mg/kg.[2] Hashimoto *et al.*[20] reported that the tacrolimus availability in the small intestine and liver were 65.7% and 38.8%, respectively. Therefore, everolimus was considered to have more difficulty in permeating the small intestine mucosa than tacrolimus in rats.

Since the therapeutic range of cyclosporine and tacrolimus early after liver transplantation is approximately 600–1,000 ng/mL at 2 hr post dose and 10 to 20 ng/mL at the trough point, respectively,[23,24] we set each dose at 5 mg/kg of cyclosporine and 1 mg/kg of tacrolimus following previous reports.[20,21] Actually, in the present study, the blood concentrations of cyclosporine and tacrolimus after 240 min were 1,458 ± 183 ng/mL and 3.8 ± 0.9 ng/mL (mean ± SE, n = 4–5) with a fluorescence polarization immunoassay method and a microparticle enzyme immunoassay method, respectively. From our results, cyclosporine significantly decreased the CL, and increased the F of everolimus after intraintestinal administration, while tacrolimus showed a less potent effect than cyclosporine. It was reported that the everolimus concentration was elevated in combination with cyclosporine in rats, in which the oral dose of cyclosporine

was 2.5 mg/kg and that of everolimus was 0.6 mg/kg.[2] Therefore, the same tendency to elevate the everolimus concentration was observed with cyclosporine in our experiments. Kovarik et al. reported that the C_{max} and AUC of everolimus was significantly elevated by 84% and 168%, respectively, in co-administration of a microemulsion formulation of cyclosporine, to healthy subjects.[13] On the other hand, concomitantly administered tacrolimus had no significant effects on the concentrations of everolimus in renal transplant patients.[25] Cyclosporine and tacrolimus competitively inhibited the CYP3A-mediated nifedipine oxidation activity with the inhibition constants of 0.36 and 1.42 μM in human liver microsomes.[26] In addition, tacrolimus stimulates the P-glycoprotein-ATPase activity with an affinity in the 100 nM range, and cyclosporine acts as a potent competitive inhibitor of verapamil-stimulated P-glycoprotein-ATPase activity with an affinity constant in the 20–25 nM range.[27] Taking these findings into consideration, lower blood concentrations of tacrolimus in the clinical situation compared with its inhibition or affinity constants for CYP3A or P-glycoprotein might have little influence on everolimus pharmacokinetics, while the blood concentrations of cyclosporine correspond to its inhibition or affinity constants. On one hand, pharmacodynamic interactions remain to be clarified in a future study because both everolimus and tacrolimus bind to FK506 binding protein (FKBP12), but the complex of everolimus and FKBP12 has no immunosuppressant effects.[1,28]

The F of everolimus was increased 1.75-fold with the concomitant administration of cyclosporine, while its CL was decreased to about 80% of the control (**Table 3**). These results showed that cyclosporine inhibited the first-pass extraction in the intestine in addition to the inhibition of hepatic extraction. To clarify the effects of calcineurin inhibitors on the intestinal and hepatic extraction of everolimus, we administered everolimus via constant intestinal or intraportal infusion for 60 min with or without calcineurin inhibitors. As a result, cyclosporine interacted with everolimus in the intestine more than in the liver, and tacrolimus did not show a significant effect (**Fig. 4**, **Table 4**). Therefore, intestinal first-pass metabolism may play an important role when considering the interaction of everolimus with CYP3A or P-glycoprotein-mediated inhibitors after oral administration. The difference between the interaction potency in the liver and intestine might be related to in part the difference in the concentration of inhibitory drugs in interaction sites, namely higher concentrations in enterocytes than in hepatocytes after oral administration. Thummel et al.[29] suggested that enzymes of the gut wall might represent an important and highly sensitive site of metabolically-based interactions for orally administed drugs, because of their unique anatomical location.

In conclusion, everolimus was extracted by the intestine to a similar extent as in the liver in rats. In addition, intraintestinally administered cyclosporine inhibited the first-pass extraction of everolimus by the intestine, rather than that by the liver in rats. It should be clarified in humans if the pharmacokinetic interaction between cyclosporine and everolimus is more evident in the intestinal first-pass extraction compared with the hepatic first-pass extraction after both drugs are orally administered.

References

1) Schuler, W., Sedrani, R., Cottens, S., Haberlin, B., Schulz, M., Schuurman, H. J., Zenke, G., Zerwes, H. G. and Schreier, M. H.: SDZ RAD, a new rapamycin derivative: pharmacological properties in vitro and in vivo. *Transplantation*, **64**: 36–42 (1997).
2) Crowe, A., Bruelisauer, A., Duerr, L., Guntz, P. and Lemaire, M.: Absorption and intestinal metabolism of SDZ-RAD and rapamycin in rats. *Drug Metab. Dispos.*, **27**: 627–632 (1999).
3) Neumayer, H. H., Paradis, K., Korn, A., Jean, C., Fritsche, L., Budde, K., Winkler, M., Kliem, V., Pichlmayr, R., Hauser, I. A., Burkhardt, K., Lison, A. E., Barndt, I. and Appel-Dingemanse, S.: Entry-into-human study with the novel immunosuppressant SDZ RAD in stable renal transplant recipients. *Br. J. Clin. Pharmacol.*, **48**: 694–703 (1999).
4) Pascual, J.: Everolimus in clinical practice–renal transplantation. *Nephrol. Dial. Transplant.*, **21** (Suppl 3): iii18–23 (2006).
5) Schweiger, M., Wasler, A., Prenner, G., Stiegler, P., Stadlbauer, V., Schwarz, M. and Tscheliessnigg, K.: Everolimus and reduced cyclosporine trough levels in maintenance heart transplant recipients. *Transplant. Immunol.*, **16**: 46–51 (2006).
6) Lehmkuhl, H., Ross, H., Eisen, H. and Valantine, H.: Everolimus (certican) in heart transplantation: optimizing renal function through minimizing cyclosporine exposure. *Transplant. Proc.*, **37**: 4145–4149 (2005).
7) Hausen, B., Boeke, K., Berry, G. J., Segarra, I., Benet, L. Z., Christians, U. and Morris, R. E.: Coadministration of neoral and the novel rapamycin analog, SDZ RAD, to rat lung allograft recipients: potentiation of immunosuppressive efficacy and improvement of tolerability of staggered versus simultaneous treatment. *Transplantation*, **67**: 956–962 (1999).
8) Kovarik, J. M., Kahan, B. D, Kaplan, B., Lorber, M., Winkler, M., Rouilly, M., Gerbeau, C., Cambon, N., Boger, R., Rordorf, C. and Everolimus Phase 2 Study Group.: Longitudinal assessment of everolimus in de novo renal transplant recipients over the first post-transplant year: pharmacokinetics, exposure-response relationships, and influence on cyclosporine. *Clin. Pharmacol. Ther.*, **69**: 48–56 (2001).
9) Crowe, A. and Lemaire, M.: In vitro and in situ absorption of SDZ-RAD using a human intestinal cell line (Caco–2) and a single pass perfusion model in rats: comparison with rapamycin. *Pharm. Res.*, **15**: 1666–1672 (1998)
10) Jacobsen, W., Serkova, N., Hausen, B., Hausen, B., Morris R. E., Benet, L. Z. and Christians, U.: Comparison of the in vitro metabolism of the macrolide immunosuppressants sirolimus and RAD. *Transplant. Proc.*, **33**: 514–515 (2001).
11) Hebert, M. F.: Contributions of hepatic and intestinal metabolism and P-glycoprotein to cyclosporine and tacrolimus oral drug delivery. *Adv. Drug Deliv. Rev.*, **27**: 201–214 (1997).
12) Mabasa, V. H. and Ensom, M. H.: The role of therapeutic

monitoring of everolimus in solid organ transplantation. *Ther. Drug Monit.*, **27**: 666–676 (2005).
13) Kovarik, J. M., Kalbag, J., Figueiredo, J., Rouilly, M., Frazier, O. L. and Rordorf, C.: Differential influence of two cyclosporine formulations on everolimus pharmacokinetics: a clinically relevant pharmacokinetic interaction. *J. Clin. Pharmacol.*, **42**: 95–99 (2002).
14) Sato, E., Shimomura, M., Masuda, S., Yano, I., Katsura, T., Matsumoto, S., Okitsu, T., Iwanaga, Y., Noguchi, H., Nagata, H., Yonekawa, Y. and Inui, K.: Temporal decline in sirolimus elimination immediately after pancreatic islet transplantation. *Drug Metab. Pharmacokinet.*, **21**: 492–500 (2006).
15) Masuda, S. and Inui, K.: An up-date review on individualized dosage adjustment of calcineurin inhibitors in organ transplant patients. *Pharmacol. Ther.*, **112**: 184–198 (2006).
16) Matsubara, T., Kim, H. J., Miyata, M., Shimada, M., Nagata, K. and Yamazoe, Y.: Isolation and characterization of a new major intestinal CYP3A form, CYP3A62, in the rat. *J. Pharmacol. Exp. Ther.*, **309**: 1282–1290 (2004).
17) Cao, X., Gibbs, S. T., Fang, L., Miller, H. A., Landowski, C. P., Shin, H. C., Lennernas, H., Zhong, Y., Amidon, G.L., Yu, L. X. and Sun, D.: Why is it challenging to predict intestinal drug absorption and oral bioavailability in human using rat model. *Pharm. Res.*, **23**: 1675–1686 (2006).
18) Venkataramanan, R., Swaminathan, A., Prasad, T., Jain, A., Zuckerman, S., Warty, V., McMichael, J., Lever, J., Burckart, G. and Starzl, T.: Clinical pharmacokinetics of tacrolimus. *Clin. Pharmacokinet.*, **29**: 404–430 (1995).
19) Ptachcinski, R. J., Venkataramanan, R. and Burckart, G. J.: Clinical pharmacokinetics of cyclosporin. *Clin. Pharmacokinet.*, **11**: 107–132 (1986).
20) Hashimoto, Y., Sasa, H., Shimomura, M. and Inui, K.: Effects of intestinal and hepatic metabolism on the bioavailability of tacrolimus in rats. *Pharm. Res.*, **15**: 1609–1613 (1998).
21) Igarashi, T., Yano, I., Saito, H. and Inui, K.: Decreased cyclosporin A concentrations in the absorption phase using microemulsion preconcentrate formulation in rats with cisplatin-induced acute renal failure. *Biol. Pharm. Bull.*, **26**: 1591–1595 (2003).
22) Laplanche, R., Meno-Tetang, G. M. and Kawai, R.: Physiologically based pharmacokinetic (PBPK) modeling of everolimus (RAD001) in rats involving non-linear tissue uptake. *J. Pharmacokinet. Pharmacodyn.*, **34**: 373–400 (2007).
23) Fukudo, M., Yano, I., Masuda, S., Fukatsu, S., Katsura, T., Ogura, Y., Oike, F., Takada, Y., Tanaka, K. and Inui, K.: Pharmacodynamic analysis of tacrolimus and cyclosporine in living-donor liver transplant patients. *Clin. Pharmacol. Ther.*, **78**, 168–181 (2005).
24) Yasuhara, M., Hashida, T., Toraguchi, M., Hashimoto, Y., Kimura, M., Inui, K., Hori, R., Inomata, Y., Tanaka, K. and Yamaoka, Y.: Pharmacokinetics and pharmacodynamics of FK506 in pediatric patients receiving living-related donor liver transplantations. *Transplant. Proc.*, **27**: 1108–1110 (1995).
25) Kovarik, J. M., Curtis, J. J., Hricik, D. E., Pescovitz, M. D., Scantlebury, V. and Vasquez, A.: Differential pharmacokinetic interaction of tacrolimus and cyclosporine on everolimus. *Transplant. Proc.*, **38**: 3456–3458 (2006).
26) Niwa, T., Yamamoto, S., Saito, M., Shiraga, T. and Takagi, A.: Effect of cyclosporine and tacrolimus on cytochrome P450 activities in human liver microsomes. *Yakugaku Zasshi.*, **127**: 209–216 (2007).
27) Rao, U. S. and Scarborough, G. A.: Direct demonstration of high affinity interactions of immunosuppressant drugs with the drug binding site of the human P-glycoprotein. *Mol. Pharmacol.*, **45**: 773–776 (1994).
28) Siekierka, J. J., Staruch, M. J., Hung, S. H. and Sigal, N. H.: FK-506, a potent novel immunosuppressive agent, binds to a cytosolic protein which is distinct from the cyclosporin A-binding protein, cyclophilin. *J. Immunol.*, **143**: 1580–1583 (1989).
29) Thummel, K. E., Kunze, K. L. and Shen, D. D.: Enzyme-catalyzed processes of first-pass hepatic and intestinal drug extraction. *Adv. Drug Deliv. Rev.*, **27**: 99–127 (1997).

Drug Metab. Pharmacokinet. 23 (5): 313–317 (2008).

Regular Article

Required Transient Dose Escalation of Tacrolimus in Living-Donor Liver Transplant Recipients with High Concentrations of a Minor Metabolite M-II in Bile

Masahiro SHIMOMURA[1], Satohiro MASUDA[1], Maki GOTO[1], Toshiya KATSURA[1], Tetsuya KIUCHI[2], Yasuhiro OGURA[2], Fumitaka OIKE[2], Yasutsugu TAKADA[2], Shinji UEMOTO[2] and Ken-ichi INUI[1,*]

[1]*Department of Pharmacy, Kyoto University Hospital, Sakyo-ku, Kyoto, Japan*
[2]*Department of Transplantation and Immunology, Graduate School of Medicine, Kyoto University, Kyoto, Japan*

Full text of this paper is available at http://www.jstage.jst.go.jp/browse/dmpk

Summary: The profiles of tacrolimus metabolites in the whole blood and bile were examined in two living-donor liver transplant patients, who transiently required higher doses of tacrolimus. Even when the 16 mg/day or oral 10 mg/day and intravenous infusion of 0.5 mg/day of tacrolimus were administered, its trough level in each patient did not reach over 15 ng/mL. By use of liquid chromatography-tandem mass spectrometry/mass spectrometry methods, a minor metabolite M-II was found to be a major metabolite both in blood and bile in these cases. However, a primary metabolite M-I was confirmed as the majority in the bile of other 8 control cases. Each graft liver and native intestine carried *CYP3A5*1/*3* or **3/*3* and **1/*3* or **1/*3*, respectively. Therefore, the *CYP3A5* genotype could not explain the present phenomena. After removing the bile drainage tube to allow the bile flow into intestine, the required doses of tacrolimus were decreased to around 20% compared to each maximum dosage. In conclusion, a minor metabolite M-II was first found in the human bile, suggesting that the appearance of M-II in bile could associate with the extensive metabolism of tacrolimus and/or the requirement of larger oral dosage.

Keywords: FK506, metabolism, pharmacokinetics, prograf

Introduction

Tacrolimus is a 23-member macrolide lactone with potent immunosuppressive properties, and has been used clinically for the prevention of rejection in organ transplantations, including living-donor liver transplantation (LDLT).[1,2] Tacrolimus is extensively metabolized in the liver by the cytochrome P450 (CYP) 3A subfamily, with little excretion of the unchanged drug in the urine, bile, or feces, and biliary excretion is thought to be the major route of elimination of tacrolimus metabolites.[3] The chemical structure of 3 major metabolites (M-I, M-II, M-III, **Fig. 1**) was determined *in vitro* with liver microsomes, however, only M-I among the three metabolites was detected in the blood of liver transplant recipients.[4,5]

Tacrolimus is a drug with a narrow therapeutic range (from 5 to 20 ng/mL), and shows large variability in bioavailability after oral administration.[6–8] Even when the blood concentration of tacrolimus is kept in the therapeutic range, patients may experience rejection episodes or adverse effects. Therefore, the pharmacological efficacy of tacrolimus is highly variable, and it is difficult to optimize the dosage and target range.[9]

In the present case report, we have retrospectively examined the whole blood and bile concentrations of tacrolimus and its three main metabolites in LDLT recipients whose blood tacrolimus concentration had been difficult to control.

Received; December 4, 2007, Accepted; February 24, 2008
**To whom correspondence should be addressed:* Prof. Ken-ichi INUI, Ph.D., *Department of Pharmacy, Kyoto University Hospital, Sakyo-ku, Kyoto 606-8507, Japan. Tel. +81-75-751-3577, Fax. +81-75-751-4207, E-mail: inui@kuhp.kyoto-u.ac.jp*
This work was supported by a Grant-in-Aid from the Japan Health Sciences Foundation "Research on Health Sciences focusing on Drug Innovation", by a Grant-in-Aid for Scientific Research from the Ministry of Education, Science, Sports, and Culture of Japan, and by the 21st Century COE program 'Knowledge Information Infrastructure for Genome Science'. M. S. is supported as a Research Fellow by the 21st Century COE program 'Knowledge Information Infrastructure for Genome Science'.

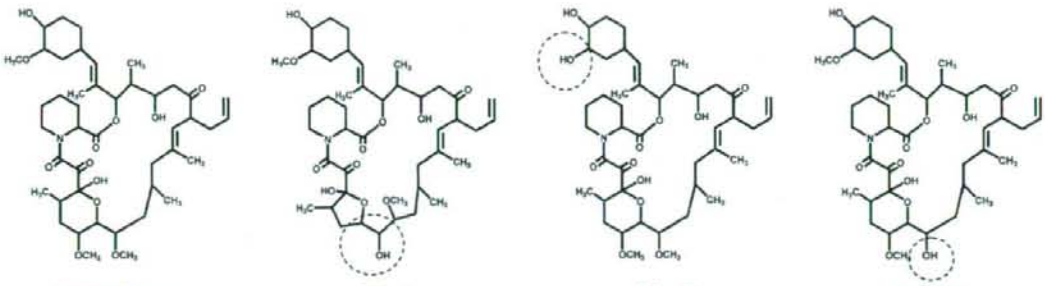

Fig. 1. Chemical structures of tacrolimus and its three metabolites.
Dotted circles indicated the positions of biotransformation.

Materials and Methods

Two LDLT patients whose tacrolimus doses were raised transiently and eight patients whose blood tacrolimus concentrations were controllable enrolled in this study after providing written informed consent. All patients had received liver transplantation at Kyoto University Hospital. The genetic analysis was performed in accordance with the Declaration of Helsinki and its amendments, and approved by Kyoto University Graduate School and Faculty of Medicine, Ethics Committee.

The blood sampling was performed once a day in the morning before the next administration of tacrolimus. The daily dose of tacrolimus was adjusted by the blood concentration of tacrolimus determined by using a semi-automated microparticle enzyme immunoassay (MEIA) (IMx®, Abbott Japan Co., Ltd., Tokyo, Japan). The excess amounts of blood samples were subjected to analyze the metabolite profile. Bile was collected from the bile drainage tube after measurement of the bile flow rate. The whole blood samples and bile samples (150 μL) were transferred to 13 mm × 100 mm conic tubes and spiked with the internal standard (25 μL, 100 ng/mL of rapamycin (Sigma-Aldrich Co., St. Louis, MO, U.S.A.)). Then, 600 μL of water and 2 mL of extraction solution (methyl-t-butyl ether/cyclohexane, 1:3 w/v) were added to the tubes. Each tube was capped securely and mixed on a horizontal shaker for 30 min, and centrifuged at 3000 rpm for 10 min. The organic layer was transferred to a clean tube, and evaporated with an Automatic Environmental Speed Vac® System (Savant Instruments, Inc., Farmingdale, NY, U.S.A.). Each tube was reconstituted with 100 μL of mobile phase and vortexed for 1 min. The concentrations of unchanged tacrolimus and its metabolites (M-I, M-II and M-III) were quantified by liquid chromatography-tandem mass spectrometry/mass spectrometry (LC-MS/MS). A 20-μL aliquot of each sample was injected into the LC-MS/MS system. Briefly, the system comprised two pumps, an analytical column (Inertsil-ODS3, 150 × 2.1 mm i.d., GL Sciences, Inc., Tokyo, Japan), and a MS/MS detector (API3000System, Applied Biosystems, CA, U.S.A.). The mobile phase consisted of a multiple gradient of solvent A (methanol/1 mM ammonium acetate) and solvent B (1 mM ammonium acetate). The flow rate was set at 250 μL/min, and the eluent was introduced directly into the electrospray ion source of the mass spectrometer. Selected reaction monitoring transitions monitored in the positive ion mode were m/z 821 → m/z 768 for tacrolimus, m/z 807 → m/z 772 for M-I, m/z 807 → m/z 754 for M-II, m/z 807 → m/z 754 for M-III, and m/z 931 → m/z 864 for rapamycin (internal standard). Tacrolimus, all metabolites, and rapamycin were detected as ammonium adducts ions ($m + NH_4$). Peak areas were linear from 0.5 to 50 ng/mL for tacrolimus and 0.5 to 20 ng/mL for metabolites.

Table 1. Patients' background

Case number	I	II
Sex	Female	Male
Age (y)	45	60
Blood type	O	O
Body weight (kg)	55.8	58.8
Primary disease	HCV-LC, HCC	HCV-LC, HCC
CYP3A5 genotype	*1/*3	*1/*3
Donor		
Relation	Husband	Son
Age (y)	49	21
Blood type	O	B
CYP3A5 genotype	*1/*3	*3/*3
ABO blood group match	Identical	Incompatible
Graft lobe	Right	Right
GRWR (%)	1.59	1.37

HCV; hepatitis virus C, LC; liver cirrhosis, HCC; hepatocellular carcinoma, GRWR; graft-to-recipient body weight ratio.

Genomic DNA from graft liver was isolated with a MagNAPure LC DNA isolation kit (Roche, Mannheim,

Germany).[10] Genotyping of the *CYP3A5* gene was performed by the polymerase chain reaction-restriction fragment length polymorphism (PCR-RFLP) method.[11,12]

Case Reports

Patients' backgrounds are shown in **Table 1**. Immunosuppression by tacrolimus was introduced with an oral administration in case I, and with an oral administration and intravenous infusion in case II. The dosage was modified mainly on the basis of the daily trough levels of tacrolimus. A small amount of prednisolone was administered for post-surgical inflammation or additional immunosuppression in both cases. During the observation period, biochemical parameters of liver function remained near the normal level in both cases (**Figs. 2A** and **3A**). By a genetic polymorphism analysis, the genotype of *CYP3A5* in the graft liver was determined as *1/*3 in case I and *3/*3 in case II. Therefore, the patients in cases I and II were classified as a CYP3A5 expressor and as CYP3A5 defective in the grafted liver, respectively. The genotype of *CYP3A5* in patients was *1/*3 in both cases, so CYP3A5 was expressed in the native intestine.

Case I: Signs of mild acute rejection were observed in the biopsy specimen, and mycophenolate mofetil (MMF) was administered from the 9th postoperative day (**Fig. 2**). This patient was discharged from our hospital on the 22nd postoperative day, and was readmitted on the 34th postoperative day with suspicion of chronic rejection. On the 44th postoperative day, the required dose of tacrolimus was raised (14 mg/day) in comparison with the mean dosage of the first 21 days post-surgery (6.5 mg/day). On the 52nd postoperative day, the bile drainage tube was removed to allow the bile to flow into

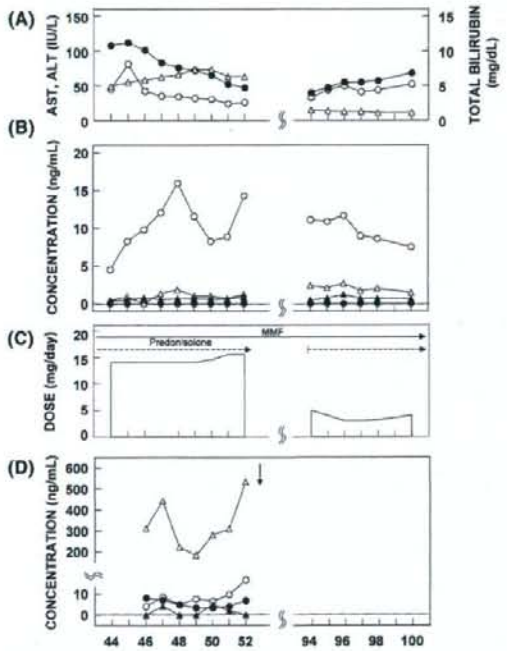

Fig. 2. Monitoring of concentrations of tacrolimus and its metabolites in whole blood and bile in case I
(A) AST (*open circle*), ALT (*closed circle*) and total bilirubin (*open triangle*) values were determined. (B) Trough tacrolimus (*open circle*), M-I (*closed circle*), M-II (*open triangle*) and M-III (*closed triangle*) levels were quantified by the LC-MS/MS method. (C) The daily oral doses of tacrolimus were documented. Arrows indicate the administration of other drugs. (D) Tacrolimus (*open circle*), M-I (*closed circle*), M-II (*open triangle*) and M-III (*closed triangle*) levels in bile were quantified by the LC-MS/MS method. The arrow indicates the time of the bile drainage tube removed.

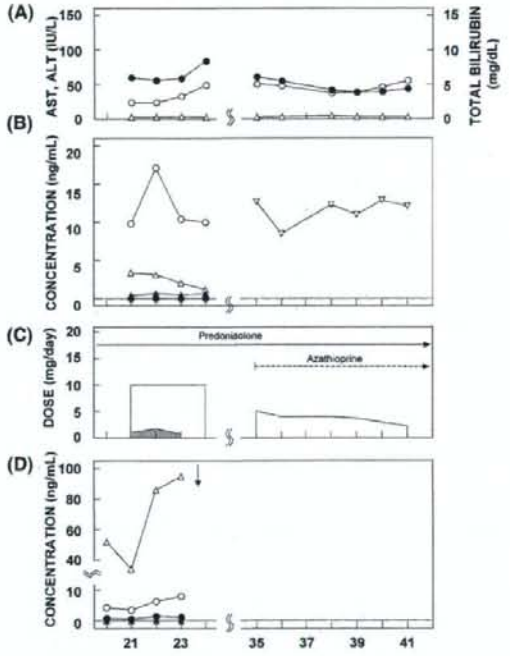

Fig. 3. Monitoring of concentrations of tacrolimus and its metabolites in whole blood and bile in case II
(A) AST (*open circle*), ALT (*closed circle*) and total bilirubin (*open triangle*) values were determined. (B) Trough tacrolimus (*open circle*), M-I (*closed circle*), M-II (*open triangle*) and M-III (*closed triangle*) levels were quantified by the LC-MS/MS method, and tacrolimus concentrations (*inverted open triangle*) were measured by MEIA method. (C) The daily oral and intravenous (*shaded area*) doses of tacrolimus were documented. Arrows indicate the administration of other drugs. (D) Tacrolimus (*open circle*), M-I (*closed circle*), M-II (*open triangle*) and M-III (*closed triangle*) levels in bile were quantified by the LC-MS/MS method. The arrow indicates the time of the bile drainage tube removed.

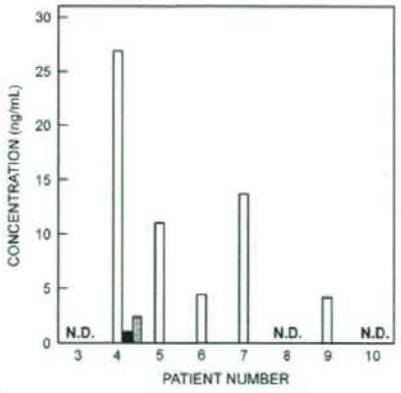

Fig. 4. Concentration of tacrolimus metabolites in the bile of 8 LDLT patients
M-I (*open column*), M-II (*solid column*) and M-III (*hatched column*) levels were quantified by the LC-MS/MS method. N.D.: not detected.

the intestine, and the required dose decreased to 3.7 mg/day, mean dosage, from the 94th to 100th postoperative day.

Case II: From the 30th postoperative day, the dose of prednisolone was decreased, and azathioprine was administered at 50 mg/day (**Fig. 3**). Although the mean dosage of tacrolimus between the 7th and 11th postoperative days was 0.62 mg/day by intravenous infusion, the required dose on the 21st postoperative day was 10 mg/day by oral administration and 0.5 mg/day by intravenous infusion. On the 24th postoperative day, the bile drainage tube was removed to allow the bile to flow into the intestine, and the required dose of tacrolimus decreased to 3.7 mg/day by oral administration only, mean dosage, from the 35th to 41st postoperative day. Because the sample volume was limited, we could not quantify the concentration of unchanged tacrolimus and its metabolite in whole blood from the 35th to 41st postoperative day. Therefore, we used the tacrolimus concentrations measured by MEIA in this period.

Control cases: The main metabolite of tacrolimus in the bile was M-I in five LDLT patients (patients 4, 5, 6, 7 and 9) who were well controlled, and no metabolite was detected in three LDLT patients with cholangitis (patients 3, 8 and 10) (**Fig. 4**). In all eight patients, unchanged tacrolimus was not detected in the bile.

Discussion

In cases I and II, after the required dose of tacrolimus was elevated in order to keep the concentration in the therapeutic range, the main metabolite was M-II in whole blood and bile (**Figs. 2** and **3**). Notably, the concentration of M-II in bile was about 10 times as high as that of unchanged tacrolimus and the other metabolites, and the concentration of M-II in whole blood was higher than that of any other metabolite. On the other hand, the main metabolite of tacrolimus in the bile was M-I in the well controlled patients (**Fig. 4**). These results indicated that the main metabolite under normal conditions was M-I, and that the profile of metabolites would change in the cases involving a remarkable elevation in dose. In addition, because only M-I among the three metabolites was reported to be in the blood,[4,5] this is the first report in which the main metabolite was found to be M-II.

Tacrolimus is extensively metabolized in the liver by CYP3A4 and CYP3A5, and biliary excretion is thought to be the major route of elimination of its metabolites.[3] CYP3A5 shows significant differences in expression caused by a single nucleotide polymorphism. The *CYP3A5*3* allele with a single nucleotide polymorphism in intron 3 causes a splicing error of CYP3A5 mRNA, and results in a defect of protein synthesis.[13,14] We previously reported that the tacrolimus concentration/dose ratio was decreased in patients engrafted with partial liver carrying the *CYP3A5*1/*1* genotype, and that intestinal CYP3A5 played an important role in the first-pass effect of orally administered tacrolimus.[8,11,12] The genotype of *CYP3A5* in native small intestine was *1/*3 in both cases (**Table 1**). It was possible that metabolism by CYP3A5 in the small intestine was responsible for high tacrolimus dose. However, the doses in both cases were elevated transiently (**Figs. 2** and **3**). Therefore, it is difficult to explain the reason for high tacrolimus dose only by intestinal metabolism by CYP3A5.

The main bile metabolite was M-II in this study, but it was reported that both CYP3A4 and 3A5 produced M-I as the main metabolite of tacrolimus.[15] Although M-II and M-III were also produced by CYP3A4 and 3A5, their amounts were 10 to 20-fold lower than that of M-I. In addition, the genotype of *CYP3A5* in the graft liver was *1/*3 in case I and *3/*3 in case II, and the high concentration of M-II is assumed not to be the result of only metabolism mediated by CYP3A5. Further study is necessary to explain the profile of tacrolimus metabolism.

The highest dose in case I was 16 mg/day. That in case II was 10 mg/day by oral administration and 0.5 mg/day by intravenous infusion. By removing the bile drainage tube, the lowest dose was reduced to 3.0 and 2.2 mg/day in cases I and II, respectively. Although it was indicated that the metabolism of tacrolimus had changed transiently in these cases, removing the bile drainage tube could assist the reabsorption of M-II, which had immunosuppressive activity, from the small intestine and enhance the immunosuppressive activity in the case of high M-II concentrations.

In conclusion, the present case report suggested that the transient elevation in the dosage of tacrolimus in the two LDLT patients was associated with the extensive for-

mation of M-II, and this is the first time the main metabolite was found to be M-II. We could decrease the dose of tacrolimus by removing the bile drainage tube. However, further investigation of many cases of LDLT and other transplantations is needed to clarify the relation of metabolites to the pharmacokinetics and pharmacodynamics of tacrolimus, because high M-II concentrations were observed in only two cases. In addition, it may be necessary to study the significance of monitoring the concentration of M-II in blood to the pharmacodynamics of tacrolimus.

Acknowledgments: We thank the Analysis and pharmacokinetics research labs of Astellas Pharma Inc. for the quantification of tacrolimus and its metabolites by LC-MS/MS.

References

1) Kiuchi, T., Inomata, Y., Uemoto, S., Asonuma, K., Egawa, H., Hayashi, M., Fujita, S. and Tanaka, K.: Living-donor liver transplantation in Kyoto, 1997. *Clin. Transpl.*, **18**: 191–198 (1997).
2) Jain, A., Reyes, J., Kashyap, R., Rohal, S., Abu-Elmagd, K., Starzl, T. and Fung, J.: What have we learned about primary liver transplantation under tacrolimus immunosuppression? Long-term follow-up of the first 1000 patients. *Ann. Surg.*, **230**: 441–449 (1999).
3) Shiraga, T., Matsuda, H., Nagase, K., Iwasaki, K., Noda, K., Yamazaki, H., Shimada, T. and Funae, Y.: Metabolism of FK506, a potent immunosuppressive agent, by cytochrome P450 3A enzymes in rat, dog and human liver microsomes. *Biochem. Pharmacol.*, **47**: 727–735 (1994).
4) Gonschior, A. K., Christians, U., Braun, F., Winkler, M., Linck, A., Baumann, J. and Sewing, K. F.: Measurement of blood concentrations of FK506 (tacrolimus) and its metabolites in seven liver graft patients after the first dose by h.p.l.c.-MS and microparticle enzyme immunoassay (MEIA). *Br. J. Clin. Pharmacol.*, **38**: 567–571 (1994).
5) Iwasaki, K.: Metabolism of tacrolimus (FK506) and recent topics in clinical pharmacokinetics. *Drug Metab. Pharmacokinet.*, **22**: 328–335 (2007).
6) Yasuhara, M., Hashida, T., Toraguchi, M., Hashimoto, Y., Kimura, M., Inui, K., Hori, R., Inomata, Y., Tanaka, K. and Yamaoka, Y.: Pharmacokinetics and pharmacodynamics of FK 506 in pediatric patients receiving living-related donor liver transplantations. *Transplant. Proc.*, **27**: 1108–1110 (1995).
7) Venkataramanan, R., Swaminathan, A., Prasad, T., Jain, A., Zuckerman, S., Warty, V., McMichael, J., Lever, J., Burckart, G. and Starzl, T.: Clinical pharmacokinetics of tacrolimus. *Clin. Pharmacokinet.*, **29**: 404–430 (1995).
8) Masuda, S. and Inui, K.: An up-date review on individualized dosage adjustment of calcineurin inhibitors in organ transplant patients. *Pharmacol. Ther.*, **112**: 184–198 (2006).
9) Fukudo, M., Yano, I., Masuda, S., Fukatsu, S., Katsura, T., Ogura, Y., Oike, F., Takada, Y., Tanaka, K. and Inui, K.: Pharmacodynamic analysis of tacrolimus and cyclosporine in patients of living donor liver transplantation. *Clin. Pharmacol. Ther.*, **78**: 168–181 (2005).
10) Goto, M., Masuda, S., Saito, H., Uemoto, S., Kiuchi, T., Tanaka, K. and Inui, K.: C3435T polymorphism in the MDR1 gene affects the enterocyte expression level of CYP3A4 rather than Pgp in recipients of living-donor liver transplantation. *Pharmacogenetics*, **12**: 451–457 (2002).
11) Goto, M., Masuda, S., Kiuchi, T., Ogura, Y., Oike, F., Okuda, M., Tanaka, K. and Inui, K.: CYP3A5*1-carrying graft liver reduces the concentration/oral dose ratio of tacrolimus in recipients of living-donor liver transplantation. *Pharmacogenetics*, **14**: 471–478 (2004).
12) Uesugi, M., Masuda, S., Katsura, T., Oike, F., Takada, Y. and Inui, K.: Effect of intestinal CYP3A5 on postoperative tacrolimus trough levels in living-donor liver transplant recipients. *Pharmacogenet. Genomics*, **16**: 119–127 (2006).
13) Kuehl, P., Zhang, J., Lin, Y., Lamba, J., Assem, M., Schuetz, J., Watkins, P. B., Daly, A., Wrighton, S. A., Hall, S. D., Maurel, P., Relling, M., Brimer, C., Yasuda, K., Venkataramanan, R., Strom, S., Thummel, K., Boguski, M. S. and Schuetz, E.: Sequence diversity in CYP3A promoters and characterization of the genetic basis of polymorphic CYP3A5 expression. *Nat. Genet.*, **27**: 383–391 (2001).
14) Lee, S. J., Usmani, K. A., Chanas, B., Ghanayem, B., Xi, T., Hodgson, E., Mohrenweiser, H. W. and Goldstein, J. A.: Genetic findings and functional studies of human CYP3A5 single nucleotide polymorphisms in different ethnic groups. *Pharmacogenetics*, **13**: 461–472 (2003).
15) Kamdem, L. K., Streit, F., Zanger, U. M., Brockmoller, J., Oellerich, M., Armstrong, V. W. and Wojnowski, J.: Contribution of CYP3A5 to the *in vitro* Hepatic Clearance of Tacrolimus. *Clin. Chem.*, **51**: 1374–1381 (2005).

BIOCHEMICAL PHARMACOLOGY 76 (2008) 894–903

available at www.sciencedirect.com

ScienceDirect

journal homepage: www.elsevier.com/locate/biochempharm

Transcellular transport of organic cations in double-transfected MDCK cells expressing human organic cation transporters hOCT1/hMATE1 and hOCT2/hMATE1

Tomoko Sato, Satohiro Masuda, Atsushi Yonezawa, Yuko Tanihara, Toshiya Katsura, Ken-ichi Inui *

Department of Pharmacy, Kyoto University Hospital, Faculty of Medicine, Sakyo-ku, Kyoto 606-507, Japan

ARTICLE INFO

Article history:
Received 23 May 2008
Accepted 1 July 2008

Keywords:
Renal tubular transport
Vectorial transport
OCT1
OCT2
MATE1
Quinidine

ABSTRACT

To clarify the transcellular transport of organic cations via basolateral and apical transporters, we established double-transfected Madin–Darby canine kidney (MDCK) cells expressing both human organic cation transporter hOCT1 and hMATE1 (MDCK-hOCT1/hMATE1), and hOCT2 and hMATE1 (MDCK-hOCT2/hMATE1) as models of human hepatocytes and renal epithelial cells, respectively. Using the specific antibodies, hOCT1 and hMATE1 or hOCT2 and hMATE1 were found to be localized in the basolateral and apical membranes of MDCK-hOCT1/hMATE1 or MDCK-hOCT2/hMATE1 cells, respectively. A representative substrate, [^{14}C]tetraethylammonium, was transported unidirectionally from the basolateral to apical side in these double transfectants. The optimal pH was showed to be 6.5 for the transcellular transport of [^{14}C]tetraethylammonium, when the pH of the incubation medium on the apical side was varied from 5.5 to 8.5. The basolateral-to-apical transport also decreased in the presence of 10 mM 1-methyl-4-phenylpyridinium or 1 mM levofloxacin on the basolateral side of both double transfectants. In MDCK-hOCT2/hMATE1 cell monolayers, but not in MDCK-hOCT1/hMATE1 cell monolayers, the accumulation of [^{14}C]tetraethylammonium was decreased in the presence of 10 mM 1-methyl-4-phenylpyridinium, but significantly increased in the presence of 1 mM levofloxacin. The uptake of [^{14}C]tetraethylammonium, [^{3}H]1-methyl-4-phenylpyridinium, [^{14}C]metformin and [^{3}H]cimetidine, but not of [^{14}C]procainamide and [^{3}H]quinidine, by HEK293 cells was stimulated by expression of the hOCT1, hOCT2 or hMATE1 compared to control cells. However, transcellular transport of [^{14}C]procainamide and [^{3}H]quinidine was clearly observed in both double-transfectants. These cells could be useful for examining the routes by which compounds are eliminated, or predicting transporter-mediated drug interaction.

1. Introduction

Renal tubular secretion of drugs, toxins and endogenous metabolites is one of the most important functions in the kidney. The characteristics of the transport of tetraethylammonium (TEA), a representative substrate of the organic cation transport system, by the basolateral and brush-border membranes revealed that transcellular transport across the renal epithelial cells was mediated by basolateral uptake from blood and subsequent extrusion from the cells into the lumen. The mechanisms of renal secretion of cationic drugs were examined using isolated membrane vesicles from rat kidney

* *Corresponding author.* Tel.: +81 75 751 3577; fax: +81 75 751 4207.
E-mail address: inui@kuhp.kyoto-u.ac.jp (K. Inui).
0006-2952/$ – see front matter © 2008 Elsevier Inc. All rights reserved.
doi:10.1016/j.bcp.2008.07.005

[1]. It was reported that the TEA transport across basolateral membranes was stimulated by an inside-negative membrane potential, and that across brush-border membranes was driven by an H^+ gradient.

Human organic cation transporter hOCT1 (SLC22A1) and hOCT2 (SLC22A2), which act as membrane potential dependent organic cation transporters, are expressed in the basolateral membranes of the liver and kidney, respectively [2]. The basolateral entry of cationic drugs is mediated mainly by hepatic hOCT1 and renal hOCT2 in humans, and hepatic Oct1 and renal Oct1 and Oct2 in mice, depending on the membrane potential [3–5]. In 2005, human multidrug and toxin extrusion 1 (hMATE1/SLC47A1) was isolated, and hMATE1 is expressed in the liver, kidney and skeletal muscle [6]. Thereafter, we identified a kidney-specific hMATE2-K (SLC47A2) [7]. Both mediated oppositely directed H^+ gradient dependent transported cationic compounds, called as H^+/organic cation antiporter, and were located in the brush-border membranes of the renal proximal tubules. Considering their characteristics, the hMATE family mediated the excretion of cationic drugs from the epithelial cells to luminal side.

Their substrate specificity, membrane localization and driving force suggested that hOCT2 and hMATE1 mediated tubular secretion of cationic drugs from blood to urine [3,7,8]. However, an in vitro model that reflects the vectorial transport of cationic drugs across human epithelial cells has not been established. Consequently, the porcine kidney epithelial cell line LLC-PK_1 has been employed to analyze transcellular transport [9,10]. These studies indicated that cationic drugs were transported unidirectionally from the basolateral to apical side in LLC-PK_1 cell monolayers. Previously, MDCK cells expressing both human organic anion transporter 8 (OATP8/SLCO1B3) and multidrug resistance protein 2 (MRP2/ABCC2) or both human organic anion-transporting polypeptide (OATP-C/SLCO1B1) and MRP2 were constructed to determine the transcellular transport of organic anions, and the vectorial transport of double-transfectants suggested their usefulness as in vitro hepatocyte models with an anion transport system [11,12].

Based on these backgrounds, it is necessary to clarify whether the basolateral hOCT1 or hOCT2 and the apical hMATE1 mediated the transcellular transport of cationic compounds. In the present study, we established MDCK cells stably expressing both hOCT2 and hMATE1 as an in vitro model of human renal epithelial cells. Human hepatocyte model expressing both hOCT1 and hMATE1 was also constructed. Moreover, the availability of these double-transfectants was evaluated to examine the transcellular transport of several cationic drugs.

2. Materials and methods

2.1. Materials

[^{14}C]Tetraethylammonium (TEA; 2.035 GBq/mmol), [^{14}C]creatinine (2.035 GBq/mmol), [^{14}C]procainamide (2.035 GBq/mmol), and [9-^{3}H]quinidine (740 GBq/mmol) were obtained from American Radiolabeled Chemicals Inc. (St. Louis, MO). [^{14}C]Metformin (962 MBq/mmol), [^{14}C]guanidine hydrochloride (1.961 GBq/mmol) and [1-^{14}C]-D-mannitol were purchased from Moravek Biochemicals Inc. (Brea, CA). [^{3}H]1-Methyl-4-phenylpyridinium acetate (MPP; 2.7 TBq/mmol) and D-[1-^{3}H(N)]-mannitol were from PerkinElmer Life Analytical Science (Boston, MA). [*N*-Methly-^{3}H]cimetidine (451 GBq/mmol) was from GE Healthcare (Buckinghamshire, UK). All other chemicals used were of the highest purity available.

2.2. Cell culture and transfection

The parental MDCK cells (ATCC CCL-34) obtained from American Type Culture Collection were cultured in complete medium consisting of Dulbecco's modified Eagle's medium (Sigma–Aldrich, St. Louis, MO) with 10% fetal bovine serum (Invitrogen, Carlsbad, CA) in an atmosphere of 5% CO_2 and 95% air at 37 8C. The hOCT1 or hOCT2 cDNA was subcloned into the Not I-cut mammalian expression vector pcDNA3.1(+) (Invitrogen). The hMATE1 cDNA was subcloned into the XbaI- and Kpn I-cut mammalian expression vector pcDNA3.1(+)/Hygro (Invitrogen). MDCK cells were cotransfected with either pcDNA3.1(+) containing hOCT1 or hOCT2 cDNA and pcDNA3.1(+)/Hygro containing hMATE1 cDNA using LipofectAMINE 2000 Reagent (Invitrogen) according to the manufacturer's instructions. Forty-eight hours later, the cells split between 1:25 and 1:100 were cultured in complete medium containing G418 (0.5 mg/ml: Nacalai Tesque Inc., Kyoto, Japan) and Hygromycin B (0.2 mg/ml; Invitrogen). Seven to fourteen days after the transfection, single colonies appeared and several G418- and Hygromycin B-resistant colonies were picked out based on the growth rate and morphology of the cells. These MDCK cells were selected on the basis of the cellular uptake of [^{14}C]TEA and named MDCK-vector (MDCK cells cotransfected with pcDNA3.1(+) empty vector and pcDNA3.1(+)/Hygro empty vector), MDCK-hOCT1/hMATE1 (MDCK cells cotransfected with pcDNA3.1(+) containing hOCT1 cDNA and pcDNA3.1(+)/Hygro containing hMATE1 cDNA) and MDCK-hOCT2/hMATE1 (MDCK cells cotransfected with pcDNA3.1(+) containing hOCT2 cDNA and pcDNA3.1(+)/Hygro containing hMATE1 cDNA). For the transcellular transport experiments, cells were seeded on microporous membrane filters [3.0-μm pores, 4.7 (or 1.0) cm^2 growth area] inside a Transwell cell culture chamber (Costar, Cambridge, MA) at a density of 5×10^5 cells/cm^2 with complete medium, as described above. In this study, MDCK cells were used between the 80th and 86th passages. HEK293 cells (American Type Culture Collection CRL-1573) were cultured as well as MDCK cells. pCMV6-XL4 plasmid vector DNA (OriGene Technologies, Rockvill, MD) that contained hOCT1 cDNA or hOCT2 cDNA or pcDNA3.1 (+)/Hygro vector DNA that contained hMATE1 cDNA was introduced into HEK293 cells using LipofectAMINE 2000 Reagent. At 48 h after the transfection, the cells were used for uptake experiment.

2.3. Polyclonal antibodies and immunofluorescence microscopy

Polyclonal antibodies were raised against the candidate peptide as described, previously [7,13]. For immunostaining, the double-transfected MDCK cells were grown 4 days in Matsunami Micro Cover Glass (Matsunami Glass Ind., Ltd., Osaka, Japan). The double-transfected MDCK cells were fixed

2% paraformaldehyde in phosphate-buffered saline (PBS) at room temperature for 10 min, and permeabilized for 5 min in 0.1% Triton X-100 in PBS. Potential sites for non-specific antibody binding were blocked by 30 min incubation with 10% FBS and 1 mg/ml RNase A (Nacalai Tesque, Kyoto, Japan) in Dulbecco's modified Eagle's medium. These cells were incubated with primary antibodies (1:200 dilution) specific for hOCT1, hOCT2, or hMATE1 for 1.5 h at room temperature. After washing with PBS, cells were incubated with the secondary antibodies (1:400 dilution) with Alexa-488-labeled phalloidin (Invitrogen) for 30 min at room temperature. All antibodies were diluted in Dulbecco's modified Eagle's medium containing 10% FBS. These cells were examined with a BX-50-FLA fluorescence microscope (Olympus, Tokyo, Japan) at 40× magnification. Images were captured with a DP-50 CCD camera (Olympus) using Studio Lite software (Olympus).

2.4. *Measurement of transcellular transport and cellular accumulation*

The transcellular transport and cellular accumulation of radiolabeled compounds by the MDCK cells were measured using monolayer cultures grown in Transwell chambers. The incubation medium for the transport experiments contained 145 mM NaCl, 3 mM KCl, 1 mM $CaCl_2$, 0.5 mM $MgCl_2$, 5 mM D-glucose and 5 mM MES (pH 5.5–6.5) or 5 mM HEPES (pH 7.0–8.5) [7]. The pH of the medium was adjusted with NaOH or HCl. In general, after the culture medium was removed from both sides of the monolayers, cells were incubated for 10 min at 37 °C with 2 ml of incubation medium (pH 7.4) on each side for the 4.7-cm^2 chamber (0.5 ml on the apical side and 1 ml on the basolateral side for the 1.0-cm^2 chamber). The incubation medium was replaced with 2 ml of incubation medium containing radiolabeled compounds on either the apical or basolateral side (1 ml in the basolateral side for the 1.0-cm^2 chamber), unlabeled incubation medium was added to the opposite side. To examine the transcellular transport, an aliquot (100 μl) of the incubation medium in the opposite side was periodically collected. To measure the cellular accumulation, the medium was immediately removed by suction at the end of the incubation period, and the monolayers were rapidly rinsed three times with 2 ml of ice-cold incubation medium (pH 7.4) in each side (1 ml each for the 1.0-cm^2 chamber). The filter was detached from the chambers, and the cells on the filters were solubilized in 0.5 ml of 0.5 N NaOH. The radioactivity of the collected medium (100 μl) and the solubilized cell monolayers (300 μl) was determined in 2 ml or 3 ml of ACSII (GE Healthcare) by liquid scintillation counting. D-[^{3}H]-mannitol or [^{14}C]-D-mannitol was used to calculate paracellular fluxes and extracellular trapping of radiolabeled compounds. The amount of protein in the solubilized cell monolayers was determined using a Bio-Rad Protein Assay kit (Bio-Rad Laboratories, Hercules, CA) with bovine γ-globulin as a standard.

2.5. *Uptake experiment*

Cellular uptake of cationic compounds was measured with HEK293 cells that were grown on poly-D-lysine-coated 24-well plates. The cells were preincubated with 0.2 ml of incubation medium for 10 min at 37 °C. After the removal of the medium, 0.2 ml of incubation medium containing the radiolabeled substrates was added. The medium was aspirated off at the end of the incubation, and the monolayers were rinsed rapidly three times with 1 ml of ice-cold incubation medium. The cells were solubilized in 0.5 ml of 0.5 N NaOH, and then the radioactivity in aliquots was determined in 3 ml of ACSII by liquid scintillation counting. For manipulation of the intracellular pH, intracellular acidification was performed by pretreatment with ammonium chloride (30 mM, 20 min at 37 °C, pH 7.4). The protein content of the solubilized cells was determined using a Bio-Rad Protein Assay Kit with bovine γ-globulin as a standard.

2.6. *Statistical analysis*

Data are expressed as means ± S.E. Data were analyzed statistically using the unpaired Student's t-test. Multiple comparisons were performed with Tukey's two-tailed test after a one-way ANOVA. Probability values of less than 0.05 were considered statistically significant.

3. Results

3.1. *Expression and localization of hOCT1, hOCT2 and hMATE1 in double-transfected MDCK cells*

The expression and localization of hOCT1, hOCT2 and hMATE1 in double transfected MDCK cells were examined by immunofluorescence microscopy. In MDCK-hOCT1/hMATE1 cells, hOCT1 and hMATE1 were localized on the basolateral and apical membrane, respectively (Fig. 1A and B). In MDCK-hOCT2/hMATE1 cells, hOCT2 was localized to the basolateral membrane, in addition to the apical appearance of hMATE1 (Fig. 1C and D). MDCK-vector cells were not observed the expression of hOCT1, hOCT2 and hMATE1 (Fig. 1E–G).

3.2. *Transcellular transport and cellular accumulation of TEA by MDCK-vector, MDCK-hOCT1/hMATE1 and MDCK-hOCT2/hMATE1 cells*

Fig. 2 shows the transcellular transport and cellular accumulation of [^{14}C]TEA from the basolateral to apical side and the apical to basolateral side by using 4.7-cm^2 chamber. The basolateral-to-apical transport was much greater than the apical-to-basolateral transport, and its rate was nearly constant for up to 60 min in MDCK-hOCT1/hMATE1 and MDCK-hOCT2/hMATE1 cell monolayers (Fig. 2B and C). The accumulation of [^{14}C]TEA from the basolateral side was 66- and 8.4-fold higher than that from the apical side in MDCK-hOCT1/hMATE1 and MDCK-hOCT2/hMATE1 cell monolayers, respectively (Fig. 2E and F). No transcellular transport or cellular accumulation of [^{14}C]TEA was observed in the MDCK-vector cell monolayers (Fig. 2A and D).

3.3. *Effect of apical pH on the transcellular transport and cellular accumulation of TEA*

Based on the functional characteristics of hMATE1 [6–8,14–19], the apical pH was suggested to be a crucial factor for its

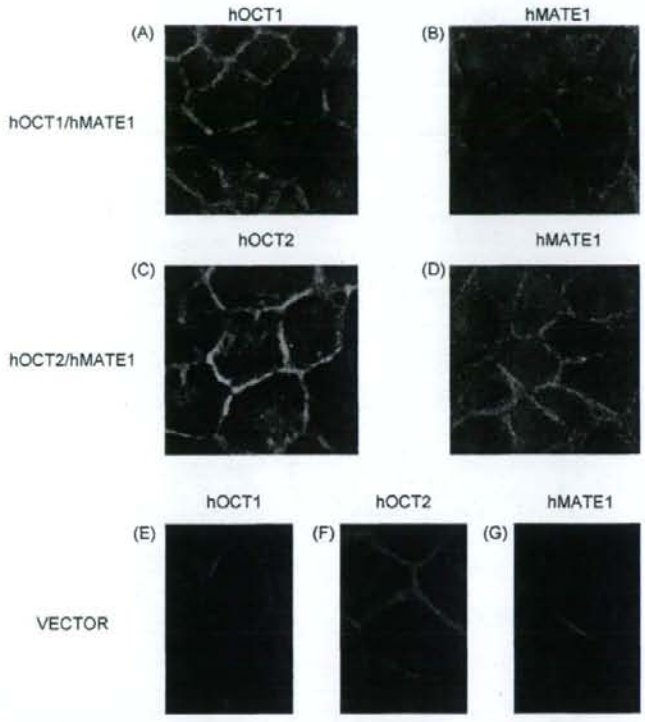

Fig. 1 – Immunofluorescence localization of hOCT and hMATE1 in the double transfected MDCK cells by immunofluorescence microscopy. MDCK-hOCT1/hMATE1 (A and B), MDCK-hOCT2/hMATE1 (C and D) and MDCK-vector (E–G) cells were stained with polyclonal antibody against hOCT1, hOCT2 or hMATE1 (red) and phalloidin (green). The yellow signals, which consist of hOCT1 or hOCT2 (red) and F-actin (green), were concentrated in basolateral side of double transfected MDCK cells (A and C). The hMATE1 expressions in double-transfected MDCK cells result in typical apical staining (B and D). No positive stainings for hOCT1, hOCT2 and hMATE1 (red) were observed in MDCK-vector cells (E–G).

transport characteristics. However, intracellular accumulation of [^{14}C]TEA was rapidly equilibrated by incubation time in MDCK-hOCT1/hMATE1 and MDCK-hOCT2/hMATE1 cell monolayers (Fig. 3E and F). Because of these technical limitations, we examined the effect of the apical pH on the transcellular transport and accumulation of [^{14}C]TEA at 5 min with 4.7-cm^2 chamber.

As shown in Fig. 4, the basolateral-to-apical transport of [^{14}C]TEA was maximal at pH 6.5 (basolateral side: pH 7.4) in MDCK-hOCT1/hMATE1 and MDCK-hOCT2/hMATE1 cell monolayers, and gradually decreased with change of the apical pH. Corresponding to the transport activity, the accumulation was increased by the alkalization of apical pH.

3.4. *Inhibitory effects of MPP and levofloxacin on the transcellular transport and cellular accumulation of TEA by MDCK-hOCT1/hMATE1 and MDCK-hOCT2/hMATE1 cells*

In MDCK-hOCT1/hMATE1 cell monolayers, the basolateral-to-apical transport and cellular accumulation of [^{14}C]TEA was decreased in the presence of 10 mM MPP or 1 mM levofloxacin at the basolateral side with 4.7-cm^2 chamber (Fig. 5B and E). In MDCK-hOCT2/hMATE1 cell monolayers, MPP and levofloxacin decreased the transcellular transport of [^{14}C]TEA (Fig. 5C). Although the presence of MPP decreased the cellular accumulation of [^{14}C]TEA, the presence of levofloxacin significantly increased the cellular accumulation of [^{14}C]TEA (Fig. 5F).

3.5. *Inhibitory effect of levofloxacin on TEA uptake by HEK293 cells expressing hOCT1, hOCT2 or hMATE1*

Fig. 6 shows the inhibitory effect of levofloxacin on [^{14}C]TEA uptake by HEK293 cells transiently expressing hOCT1, hOCT2 or hMATE1. In the HEK293 cells expressing hOCT1 or hMATE1, the presence of levofloxacin markedly reduced the uptake of [^{14}C]TEA. In contrast, the [^{14}C]TEA uptake in the hOCT2 expressing cells was not changed with or without levofloxacin.

3.6. *Uptake of various cationic compounds in HEK293 cells transfected with hOCT1, hOCT2 or hMATE1*

Prior to experiment with double transfectants, the uptake of various organic cations by hOCT1, hOCT2 or hMATE1 was examined. The uptake of [^{14}C]TEA, [^{3}H]MPP, [^{14}C]metformin

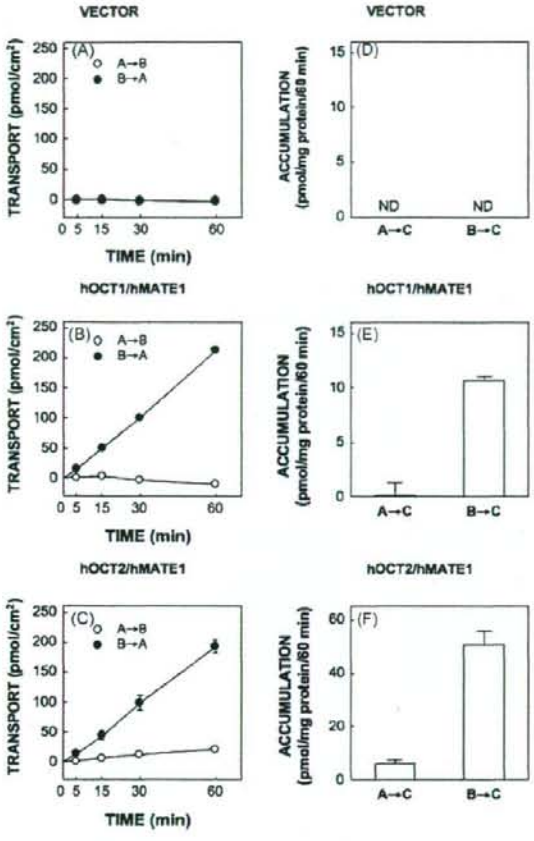

Fig. 2 – Transcellular transport (A–C) and cellular accumulation (D–F) of [^{14}C]TEA in MDCK-vector (A and D), MDCK-hOCT1/hMATE1 (B and E) and MDCK-hOCT2/hMATE1 (C and F) cell monolayers in 4.7-cm^2 chamber. The cells were incubated in medium containing 5 μM [^{14}C]TEA added to the basolateral (closed circle) or apical (open circle) side. The radioactivity on the opposite side was periodically measured. After a 60-min incubation, the radioactivity of solubilized cells was measured. Each point or column represents the mean ± S.E. for three monolayers from a typical experiment. N.D., not detected.

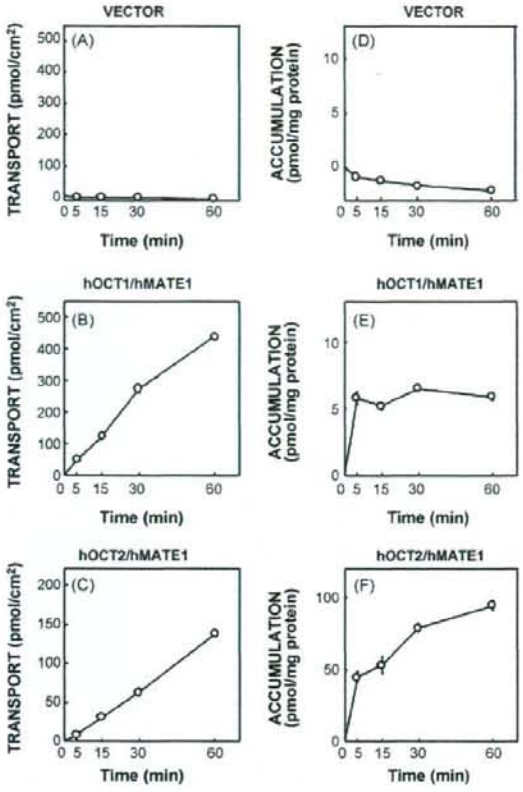

Fig. 3 – Time course of [^{14}C]TEA accumulation by MDCK-vector (A and D), MDCK-hOCT1/hMATE1 (B and E) and MDCK-hOCT2/hMATE1 (C and F) cell monolayers in 1.0-cm^2 chamber. The cells were incubated in medium containing 5 μM TEA added to the basolateral side. The radioactivity in the apical medium and solubilized cells were measured at the end of incubation. Each point represents the mean ± S.E. for three monolayers from a typical experiment.

and [^{3}H]cimetidine was markedly stimulated in hOCT1- and hOCT2-expressing cells (Table 1). The uptake of [^{14}C]creatinine and [^{14}C]guanidine was significantly increased in hOCT2-expressing cells, but not in hOCT1-expressing cells. [^{14}C]Procainamide and [^{3}H]quinidine were transported by hOCT1. Although [^{14}C]procainamide was also recognized, [^{14}C]quinidine was slightly, but not significantly, transported by hOCT2. hMATE1 extensively transported [^{14}C]TEA, [^{3}H]MPP, [^{14}C]metformin, [^{3}H]cimetidine, [^{14}C]creatinine and [^{14}C]procainamide after the pre-treatment with ammonium chloride (Table 2). The cellular accumulation of [^{14}C]guanidine and [^{3}H]quinidine was weakly but significantly increased in hMATE1-expressing cells compared to control cells.

3.7. *Transcellular transport and cellular accumulation of various cationic compounds*

Because the sum of the basolateral uptake and apical secretion of organic cations was supposed to reflect the in vivo biliary and tubular secretion, we examined the transcellular transport of these compounds using the established double transfectants with 1.0-cm^2 chamber (Tables 3 and 4). The basolateral-to-apical transport of [^{14}C]TEA, [^{3}H]MPP, [^{14}C]metformin, [^{3}H]cimetidine, [^{14}C]procainamide and [^{3}H]quinidine was much greater than the apical-to-basolateral transport by MDCK-hOCT1/hMATE1

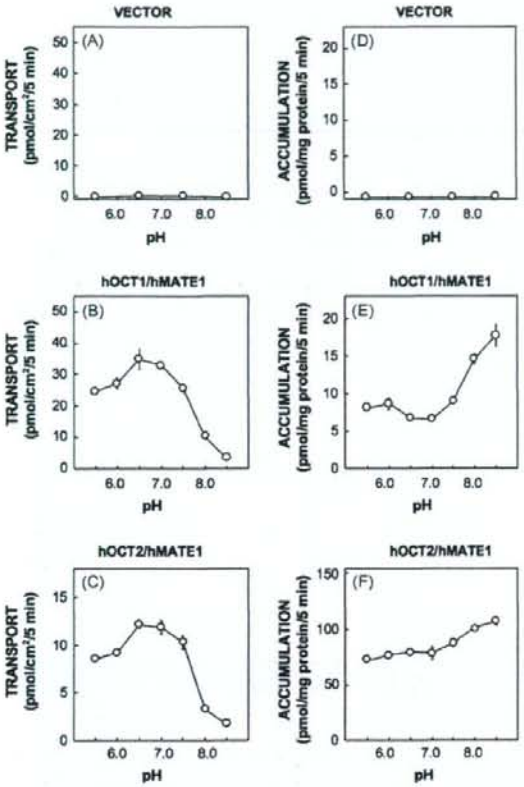

Fig. 4 – Effect of apical pH on the transcellular transport (A–C) and cellular accumulation (D–F) of [^{14}C]TEA in MDCK-vector (A and D), MDCK-hOCT1/hMATE1 (B and E), and MDCK-hOCT2/hMATE1 (C and F) cell monolayers in 4.7-cm^2 chamber. The cells were incubated in medium containing 5 μM [^{14}C]TEA added to the basolateral side for 5 min. The pH of the apical medium was between 5.5 and 8.5, and that of the basolateral medium was 7.4. The radioactivity in the apical medium and solubilized cells were measured at the end of incubation. Each point represents the mean ± S.E. for three monolayers from a typical experiment.

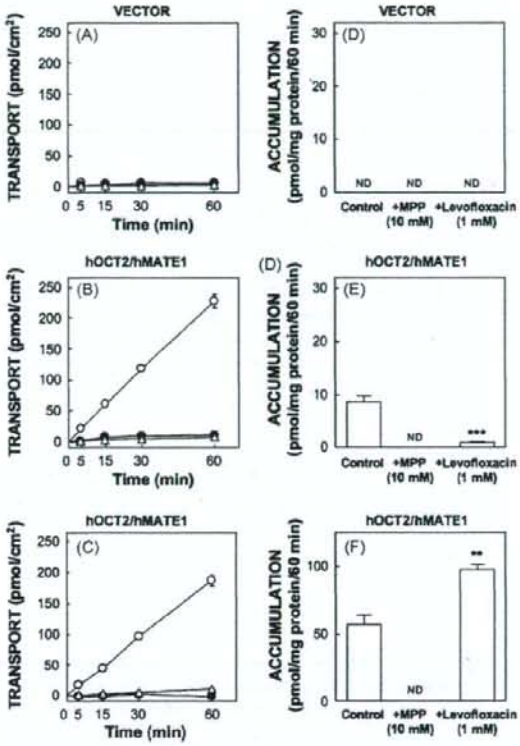

Fig. 5 – Effect of MPP and levofloxacin on the transcellular transport (A–C) and cellular accumulation (D–F) of [^{14}C]TEA in MDCK-vector (A and D), MDCK-hOCT1/hMATE1 (B and E), and MDCK-hOCT2/hMATE1 (C and F) cell monolayers in 4.7-cm^2 chamber. These cell monolayers were incubated in medium containing 5 μM [^{14}C]TEA added to the basolateral side in the absence (control, open circle) or presence of 10 mM MPP (+MPP, closed circle) or 1 mM levofloxacin (+levofloxacin, open triangle). The pH of the basolateral and apical incubation medium was 7.4 and 6.0, respectively. The radioactivity on the apical side was periodically measured. After a 60-min incubation, the radioactivity of solubilized cells was measured. Each symbol and column represents the mean ± S.E. for three monolayers from a typical experiment. N.D., not detected. **$P < 0.01$ and ***$P < 0.001$ significantly different from control cells.

and MDCK-hOCT2/hMATE1 cell monolayers (Tables 3 and 4). In the MDCK-hOCT1/hMATE1 cell monolayers, the cellular accumulation of these compounds was greater from the basolateral side than apical side (Table 3). Although the transcellular transport of [^{14}C]creatinine and [^{14}C]guanidine was slightly increased in MDCK-hOCT1/hMATE1 cell monolayers, there was no difference between apical-to-basolateral and basolateral-to-apical transport in the MDCK-hOCT2/hMATE1 cell monolayers. On the other hand, the cellular accumulation was also greater from the basolateral than apical side (Tables 3 and 4).

4. Discussion

The functional characterization of MATE1 and MATE2-K as the apical H^+/organic cation antiporter has been examined using transfected cells and isolated membrane vesicles [7,8,14–16,18,19]. However, most of the characteristics of MATE transporters were determined in the direction of uptake using an oppositely directed H^+ gradient. Therefore, examination of the H^+/organic cation antiport functions of MATE transporters

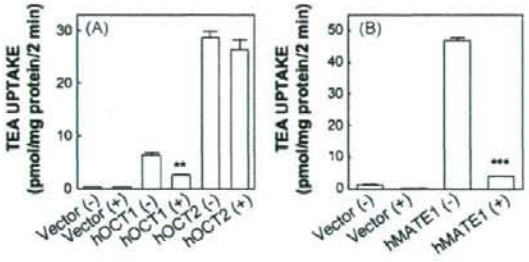

Fig. 6 – Effect of levofloxacin on the uptake of [^{14}C]TEA by HEK293 cells transiently expressing hOCT1, hOCT2 (A) and hMATE1 (B). The cells were incubated with medium containing 5 μM [^{14}C]TEA in the absence (–) or presence (+) of 1 mM levofloxacin at pH 7.4 for 2 min. For intracellular acidification, hMATE1 expressing cells were preincubated in medium containing 30 mM ammonium chloride for 20 min (B). The amount of substrate in the cells was determined by measuring the radioactivity of solubilized cells. Each column represents the mean ± S.E. for three monolayers. **P < 0.01 and ***P < 0.001 significantly different from the uptake of the absence of levofloxacin. .

in the direction of efflux has been considered to be difficult. The extracellular H^+ concentration-dependent efflux of pre-loaded TEA was showed by the CHO cells expressing rabbit (rb) MATE1 and rbMATE2-K [17]. However, it may be difficult to examine the efflux activity with lipophilic compounds in this method. We hypothesized that the "efflux-function" via MATE transporters can be revealed in polarized epithelial cells with the basolateral OCT system regardless of the lipophilicity of compounds. In the present study, we have successfully established double-transfected MDCK cells expressing both hOCT1 and hMATE1 or both hOCT2 and hMATE1 as an in vitro model of the organic cation transport system in the human hepatocyte and human tubular epithelial cell, respectively.

Typical and hydrophilic substrates for organic cation transporters, [^{14}C]TEA, [^{3}H]MPP, [^{14}C]metformin and [^{3}H]cimetidine were strongly transported by the HEK293 cells expressing either hOCT1, hOCT2 or hMATE1 (Tables 1 and 2). Indeed, metformin and cimetidine were indicated to be eliminated by renal tubular secretion [20–22], and the molecular mechanisms of renal secretion were revealed to be mediated by organic cation transport systems [8,23]. In the MDCK-hOCT2/hMATE1 cell monolayers, the unidirectional transcellular transport of these compounds from the basolateral to apical

Table 1 – Uptake of cationic compounds by HEK293 cells expressing hOCT1 or hOCT2

Cationic compounds	Vector (μl/mg protein/2 min)	hOCT1 (μl/mg protein/2 min)	hOCT2 (μl/mg protein/2 min)
[^{14}C]TEA	0.08 ± 0.00	2.64 ± 0.03**	2.86 ± 0.09**
[^{3}H]MPP	1.01 ± 0.01	8.72 ± 0.47**	7.17 ± 0.51**
[^{14}C]Metformin	0.18 ± 0.01	0.72 ± 0.04**	4.01 ± 0.08**
[^{3}H]Cimetidine	0.49 ± 0.02	0.86 ± 0.01**	1.31 ± 0.02**
[^{14}C]Creatinine	0.98 ± 0.01	0.93 ± 0.05	2.27 ± 0.09**
[^{14}C]Guanidine	2.23 ± 0.06	2.11 ± 0.07	5.71 ± 0.19**
[^{14}C]Procainamide	3.36 ± 0.18	5.13 ± 0.09**	5.32 ± 0.28**
[^{3}H]Quinidine	37.4 ± 0.43	47.8 ± 3.43*	43.4 ± 1.12

HEK293 cells were transfected with the empty vector, hOCT1 cDNA or hOCT2 cDNA. The cells were incubated with medium containing 5 μM [^{14}C]TEA 15 nM [^{3}H]MPP, 10 μM [^{14}C]metformin, 92 nM [^{3}H]cimetidine, 5 μM [^{14}C]creatinine, 5 μM [^{14}C]guanidine, 5 μM [^{14}C]procainamide and 56 nM [^{3}H]quinidine at pH 7.4 for 2 min. The amount of substrate in the cells was determined by measuring the radioactivity of solubilized cells. Date represents the mean ± S.E. for three monolayers. TEA, tetraethylammonium; MPP, 1-methyl-4-phenylpyridinium acetate.

* $P < 0.05$.

** $P < 0.01$ significantly different from vector-transfected cells.

Table 2 – Uptake of cationic compounds by HEK293 cells expressing hMATE1

Cationic compounds	Vector (μl/mg protein/2 min)	hMATE1 (μl/mg protein/2 min)
[^{14}C]TEA	0.09 ± 0.00	15.9 ± 0.34***
[^{3}H]MPP	0.85 ± 0.03	40.3 ± 1.36***
[^{14}C]Metformin	0.18 ± 0.01	24.9 ± 0.77***
[^{3}H]Cimetidine	0.53 ± 0.00	9.27 ± 0.38***
[^{14}C]Creatinine	0.41 ± 0.02	2.41 ± 0.11**
[^{14}C]Guanidine	1.36 ± 0.03	2.77 ± 0.27*
[^{14}C]Procainamide	6.78 ± 0.29	18.8 ± 0.41***
[^{3}H]Quinidine	38.9 ± 0.49	46.2 ± 0.37**

HEK293 cells transfected with the empty vector or hMATE1 cDNA. The cells were preincubated in medium containing 30 mM ammonium chloride for 20 min to make an intracellular acidification, and then incubated in medium containing radiolabeled compounds as described in the legend for Table 1. Data represents the mean ± S.E. for three monolayers.

** $P < 0.01$.

*** $P < 0.001$ significantly different from vector-transfected cells.

Table 3 – Transcellular transport and cellular accumulation of various cationic compounds in MDCK-hOCT1/hMATE1 cell monolayers

Cationic compounds	Transport (μl/cm²/30 min)		Accumulation (μl/mg protein/30 min)	
	A → B	B → A	A → C	B → C
[¹⁴C]TEA	N.D.	23.7 ± 0.64‴	N.D.	1.92 ± 0.07‴
[³H]MPP	5.40 ± 0.24	117 ± 2.58‴	0.49 ± 0.02	2.40 ± 0.04‴
[¹⁴C]Metformin	2.17 ± 0.30	31.3 ± 0.59‴	0.11 ± 0.04	2.13 ± 0.19‴
[³H]Cimetidine	1.67 ± 0.61	49.4 ± 1.06‴	0.79 ± 0.04	1.51 ± 0.10‴
[¹⁴C]Creatinine	1.94 ± 0.27	3.19 ± 0.11*	N.D.	0.83 ± 0.08‴
[¹⁴C]Guanidine	14.5 ± 0.33	22.5 ± 0.35‴	0.11 ± 0.08	2.49 ± 0.27‴
[¹⁴C]Procainamide	N.D.	27.4 ± 2.09‴	0.19 ± 0.04	1.12 ± 0.06‴
[³H]Quinidine	0.48 ± 0.30	95.0 ± 1.07‴	18.2 ± 0.32	51.3 ± 2.61‴

The cells were incubated in medium containing radiolabeled compounds added to the basolateral (B → A) or apical (A → B) side as described in the legend for Table 1. The radioactivity in the opposite side and solubilized cells (C) was measured at the end of incubation. Data represents the mean ± S.E. for three monolayers from typical experiments. N.D., not detected.

* $P < 0.05$.

‴ $P < 0.001$ significantly different from apical to basolateral (transport) or apical to cell (accumulation).

Table 4 – Transcellular transport and cellular accumulation of various cationic compounds in MDCK-hOCT2/hMATE1 cell monolayers

Cationic compounds	Transport (μl/cm²/30 min)		Accumulation (μl/mg protein/30 min)	
	A → B	B → A	A → C	B → C
[¹⁴C]TEA	0.63 ± 0.34	19.8 ± 0.57‴	0.33 ± 0.27	14.0 ± 0.36‴
[³H]MPP	10.3 ± 0.33	120 ± 2.20‴	1.71 ± 0.03	11.8 ± 0.72‴
[¹⁴C]Metformin	0.23 ± 0.07	15.0 ± 0.60‴	0.04 ± 0.04	13.6 ± 0.28‴
[³H]Cimetidine	N.D.	17.9 ± 0.48‴	0.22 ± 0.04	5.85 ± 0.28‴
[¹⁴C]Creatinine	1.84 ± 0.20	1.80 ± 0.07	N.D.	1.43 ± 0.09‴
[¹⁴C]Guanidine	14.2 ± 3.14	18.7 ± 0.10	1.63 ± 0.43	11.2 ± 0.31‴
[¹⁴C]Procainamide	N.D.	9.06 ± 0.27‴	0.15 ± 0.04	4.30 ± 0.23‴
[³H]Quinidine	1.23 ± 0.21	72.9 ± 5.27‴	18.5 ± 0.55	77.8 ± 4.31‴

The cells were incubated in medium containing radiolabeled compounds added to the basolateral (B → A) or apical (A → B) side as described in the legend for Table 1. The radioactivity in the opposite side and solubilized cells (C) was measured at the end of incubation. Data represents the mean ± S.E. for three monolayers from typical experiments. N.D., not detected.

‴ $P < 0.01$.

‴ $P < 0.001$ significantly different from apical to basolateral (transport) or apical to cell (accumulation).

side was observed, corresponding to the tubular secretion (Table 4). These results suggested that MDCK-hOCT2/hMATE1 cell monolayers successfully reproduced the renal tubular secretion, and this transfectant can be used to examine the tubular secretion via the human organic cation transport system. The MDCK-hOCT1/hMATE1 cell monolayers also showed the unidirectional transcellular transport of [¹⁴C]TEA, [³H]MPP, [¹⁴C]metformin and [³H]cimetidine from the basolateral side, corresponding to biliary excretion (Table 3). Considering the in vivo pharmacokinetics of cimetidine and metformin [21,22], the present results suggest that intestinal reabsorption of these drugs after biliary secretion may have occurred. Although the report that MDCK cells originally expressed an OCT on basolateral side [24], MDCK-vector cell monolayers in the present study did not show the transcellular transport and accumulation of [¹⁴C]TEA (Fig. 2A and D). In addition, we previously examined that the radioactivity of [¹⁴C]TEA added to the basolateral side was not transported to the apical side, in the MDCK cells stably expressing rat OCT1 and OCT2 (data not shown) [25], and then, the function corresponding to hMATE1 was indicated to be lacked in MDCK cells. Therefore, we consider that MDCK cells in the present study were not expressing an original OCT on basolateral side.

Immunostaining against hOCT1 or hOCT2 in double transfected MDCK cells was observed as yellow signals merged with green phalloidin and red antibodies (Fig. 1A and C). Despite the red staining was observed at the intracellular space of MDCK-hOCT1/hMATE1 and MDCK-hOCT2/hMATE1 cells, they were considered to be non-specific signals from the functional analysis. Therefore, we confirmed that hOCT1 and hOCT2 were localized on the basolateral side, and hMATE1 on the apical side in double-transfected MDCK cells.

The uptake experiments using HEK293 cells expressing hOCT1, hOCT2 or hMATE1 gave results that contradicted the in vivo data in the cases of procainamide and quinidine, the lipophilic cations. In the human pharmacokinetic analysis, the renal clearance of procainamide was decreased by the coadministration of cimetidine [26] and the renal clearance of unbound quinidine was greater than the clearance of creatinine [27]. These reports suggested that procainamide

and quinidine undergo active tubular secretion in the human kidney. In uptake experiments, the accumulation of [^{14}C]procainamide and [^{3}H]quinidine by HEK293 cells expressing hOCT1, hOCT2 or hMATE1 was not so great compared to that by vector-transfected control cells, unlike in the case of [^{14}C]metformin and [^{3}H]cimetidine (Tables 1 and 2). These results could not clearly indicate that the renal secretion of procainamide and quinidine was mediated by the organic cation transport system. In the transcellular transport experiments with MDCK-hOCT1/hMATE1 and MDCK-hOCT2/hMATE1 cell monolayers, clear directional transport of [^{14}C]procainamide and [^{3}H]quinidine was observed from the basolateral to apical side, corresponding to biliary excretion and renal tubular secretion (Tables 3 and 4). These results suggested that the biliary excretion and renal tubular secretion of procainamide and quinidine are involved in the basolateral uptake by hOCT and apical efflux by hMATE1 in humans. Because uptake experiments can not discriminate between the specific intracellular accumulation by transporters and non-specific binding to the cell surface and/or diffusion dependent on lipophilicity, it was considered that such experiments alone could not clarify the tubular secretion of procainamide and quinidine via the organic cation transport system. The double-transfected MDCK-hOCT1/hMATE1 and MDCK-hOCT2/hMATE1 cells clearly solved these technical limitations of the uptake experiments, and would be useful in vitro tools to examine the biliary and renal tubular secretion of cationic drugs in humans.

In the liver, the existence of the H^+/organic cation antiporter has been examined using canalicular membrane vesicles [28]. In this report, an outwardly directed H^+ gradient stimulated the TEA uptake by canalicular membrane vesicles, suggesting that organic cation transport across the hepatic canalicular membranes is mediated by the H^+/organic cation antiporter. Consistent with this report, hMATE1 is expressed in the liver as well as kidney [6]. In contrast, the source of the H^+ gradient is considered to differ between the kidney and the liver. In the brush-border membranes of renal proximal tubules, the Na^+/H^+ antiporter NHE3 and H^+-ATPase are considered to produce an inward H^+ gradient [29,30]. However, the Na^+/H^+ exchanger is not functional in the canalicular membranes in the liver [31,32]. It remains unclear whether hMATE1 functions well in the liver like in the kidney. A comparison between the in vivo hepatic pharmacokinetics and the transcellular transport by the MDCK-hOCT1/hMATE1 cells may be revealed the physiological significance of hepatic hMATE1 as a detoxicating molecule.

Previously, we found that the new-quinolone antibiotics ofloxacin and levofloxacin strongly inhibited the transport of TEA via the H^+/organic cation antiport system using the isolated rat renal brush-border membrane vesicles and the LLC-PK_1 cell monolayers [33,34]. Moreover, we have reported that levofloxacin inhibited the transport of [^{14}C]TEA by hMATE1 [8], but not by hOCT2 [35]. However, the effect of levofloxacin on the renal handling of cationic drugs in humans has not been elucidated. In the MDCK-hOCT2/hMATE1 cell monolayers, the transcellular transport of [^{14}C]TEA was markedly decreased in the presence of 10 mM MPP and 1 mM levofloxacin in the basolateral chamber (Fig. 5C). On the other hand, the cellular accumulation of [^{14}C]TEA was decreased by MPP and increased by levofloxacin (Fig. 5F). In MDCK-hOCT1/hMATE1 cell monolayers, the transcellular transport and accumulation of [^{14}C]TEA was inhibited by 10 mM MPP and 1 mM levofloxacin (Fig. 5B and E). Considering the results by the single transfectants of hOCT1, hOCT2 and hMATE1 (Fig. 6), these results in the MDCK-hOCT2/hMATE1 monolayers suggested that levofloxacin selectively inhibited the transport of [^{14}C]TEA by apical hMATE1 rather than basolateral hOCT2, and therefore, coadministration of levofloxacin may increase the tubular accumulation of cationic drugs and the risk of subsequent drug-induced nephrotoxicity.

hMATE2-K as well as hMATE1 was found in the human kidney, and both transporters were suggested to play important roles in the urinary secretion of cationic compounds [7]. Although these transporters have a similar substrate specificity, some differences were found. The amino beta-lactam antibiotic cephalexin was preferentially transported by hMATE1, and the anticancer agent oxaliplatin was by hMATE2-K [8,15]. However, the substrate specificity was mainly examined with uptake experiments. Because hMATE1 and hMATE2-K act as efflux transporters, the construction of MDCK cells expressing basolateral hOCT2 and apical hMATE2-K will be required in future. A comparison of substrate specificity between hMATE1 and hMATE2-K for basolateral-to-apical transport using double transfectants would clearly distinguish the physiological characteristics of these two transporters.

In conclusion, we have successfully established double-transfected MDCK cells expressing both hOCT1 and hMATE1 or both hOCT2 and hMATE1. These double transfectants represented the vectorial transcellular transport of cationic drugs elucidating at least a part of the molecular mechanisms of hepatic- and/or renal-handling of cationic drugs in humans. The MDCK-hOCT1/hMATE1 and MDCK-hOCT2/hMATE1 cells are suggested to be useful for determining the routes by which newly synthesized cationic compounds are eliminated, or predicting transporter-mediated drug interaction in humans.

Acknowledgements

This work was supported in part by a grant-in-aid for Research on Biological Markers for New Drug Development, Health and Labour Sciences Research Grants from the Ministry of Health, Labour and Welfare of Japan, by the Mochida Memorial Foundation for Medical and Pharmaceutical Research, and by a grant-in-aid for Scientic Research from the Ministry of Education, Science, Culture and Sports of Japan.

REFERENCES

[1] Takano M, Inui K, Okano T, Saito H, Hori R. Carrier-mediated transport systems of tetraethylammonium in rat renal brush-border and basolateral membrane vesicles. Biochim Biophys Acta 1984;773:113–24.
[2] Gorboulev V, Ulzheimer JC, Akhoundova A, Ulzheimer-Teuber I, Karbach U, Quester S, et al. Cloning and characterization of two human polyspecific organic cation transporters. DNA Cell Biol 1997;16:871–81.